Neuropsychopharmacology (2010) 35, 806–817
© 2010 Nature Publishing Group All rights reserved 0893-133X/10 $32.00
www.neuropsychopharmacology.org

Impact of D2 Receptor Internalization on Binding Affinity of Neuroimaging Radiotracers

Ningning Guo[1,2], Wen Guo[3], Michaela Kralikova[3], Man Jiang[1,4], Ira Schieren[5], Raj Narendran[1,2], Mark Slifstein[1,2], Anissa Abi-Dargham[1,2], Marc Laruelle*[,1,6,7], Jonathan A Javitch*[,1,3,4] and Stephen Rayport*[,1,4]

[1]Department of Psychiatry, Columbia University, New York, NY, USA; [2]Department of Translational Imaging, New York State Psychiatric Institute, New York, NY, USA; [3]Center for Molecular Recognition, Columbia University, New York, NY, USA; [4]Department of Molecular Therapeutics, New York State Psychiatric Institute, New York, NY, USA; [5]Howard Hughes Medical Institute, Columbia University, New York, NY, USA; [6]Neurosciences Center for Excellence in Drug Discovery, GlaxoSmithKline, London, UK; [7]Department of Neuroscience, Imperial College, London, UK

Synaptic dopamine (DA) levels seem to affect the *in vivo* binding of many D2 receptor radioligands. Thus, release of endogenous DA induced by the administration of amphetamine decreases ligand binding, whereas DA depletion increases binding. This is generally thought to be due to competition between endogenous DA and the radioligands for D2 receptors. However, the temporal discrepancy between amphetamine-induced increases in DA as measured by microdialysis, which last on the order of 2 h, and the prolonged decrease in ligand binding, which lasts up to a day, has suggested that agonist-induced D2 receptor internalization may contribute to the sustained decrease in D2 receptor-binding potential seen following a DA surge. To test this hypothesis, we developed an *in vitro* system showing robust agonist-induced D2 receptor internalization following treatment with the agonist quinpirole. Human embryonic kidney 293 (HEK293) cells were stably co-transfected with human D2 receptor, G-protein-coupled receptor kinase 2 and arrestin 3. Agonist-induced D2 receptor internalization was demonstrated by fluorescence microscopy, flow cytometry, and radioligand competition binding. The binding of seven D2 antagonists and four agonists to the surface and internalized receptors was measured in intact cells. All the imaging ligands bound with high affinity to both surface and internalized D2 receptors. Affinity of most of the ligands to internalized receptors was modestly lower, indicating that internalization would reduce the binding potential measured in imaging studies carried out with these ligands. However, between-ligand differences in the magnitude of the internalization-associated affinity shift only partly accounted for the data obtained in neuroimaging experiments, suggesting the involvement of mechanisms beyond competition and internalization.

Neuropsychopharmacology (2010) **35,** 806–817; doi:10.1038/npp.2009.189; published online 2 December 2009

Keywords: DA; raclopride; sulpiride; imaging; endogenous competition; HEK293 cells

INTRODUCTION

Many studies have shown that acute fluctuations in synaptic dopamine (DA) affect the *in vivo* binding of D2 receptor radioligands used in single photon emission computed tomography (SPECT) and positron emission tomography (PET) studies (for review, see Laruelle, 2000). An increase in DA release, such as that induced by amphetamine administration, leads to an acute decrease in the *in vivo* binding of imaging ligands. Conversely, reducing DA release by DA depletion leads to an increase in the *in vivo* binding of the ligands. The recognition of this phenomenon in animals inspired the methodology to measure changes in synaptic DA in humans with SPECT using IBZM and with PET using raclopride. This methodology has been used extensively to study alterations in DA transmission in schizophrenia (Laruelle *et al*, 1996; Breier *et al*, 1997; Abi-Dargham *et al*, 2000) and substance abuse (Volkow *et al*, 1997; Martinez *et al*, 2007), as well as the effects of stimulants on DA neurotransmission (Kegeles *et al*, 2000; van Berckel *et al*, 2006; Volkow *et al*, 2009).

The ability of neuroimaging ligands to report on changes in synaptic DA has been validated by two key observations. In humans, DA depletion blocks the effect of stimulants on the *in vivo* binding of PET radiotracers (Laruelle *et al*, 1997a). In nonhuman primates, the magnitude of DA release, as measured with microdialysis, correlates with the decrease in D2 receptor-binding potential (BP, the ratio of receptor number to affinity, B_{max}/K_D), as measured with PET or SPECT (Breier *et al*, 1997; Laruelle *et al*, 1997b). These interactions have been reliably observed

*Correspondence: Dr S Rayport or Dr JA Javitch or Dr M Laruelle, Department of Psychiatry, Columbia University, 1051 Riverside Drive, NYSPI Unit 62, New York, NY 10032, USA, Tel: +1 212 543 5641, Fax: +1 212 504 3135, E-mail: sgr1@columbia.edu or jaj2@columbia.edu or m.laruelle@imperial.ac.uk
Received 1 September 2009; revised 21 October 2009; accepted 22 October 2009

with moderate-to-high-affinity D2 receptor benzamide antagonists, [^{11}C]raclopride ($K_D = 1$ nM), [^{123}I]IBZM ($K_D = 0.2$ nM), and [^{18}F]fallypride ($K_D = 0.2$ nM) (Laruelle, 2000; Slifstein *et al*, 2004; Mukherjee *et al*, 2005; Riccardi *et al*, 2006; Cropley *et al*, 2008; Narendran *et al*, 2009), but inconsistently with the very-high-affinity D2 receptor antagonists, [^{11}C]*N*-methylspiperone ([^{11}C]NMSP, $K_D = 0.07$ nM), [^{11}C]FLB457 ($K_D = 0.03$ nM), and [^{123}I]epidepride ($K_D = 0.01$ nM) (Laruelle, 2000; Aalto *et al*, 2009; Narendran *et al*, 2009). This divergence may be due to physiochemical differences among the ligands, or because of the technical difficulties encountered in quantification of striatal D2 receptor availability with very-high-affinity ligands. Studies with the radiolabeled D2 receptor agonists, [^{11}C]NPA and [^{11}C]PHNO, have shown that the *in vivo* binding of these tracers is also sensitive to changes in synaptic DA (Narendran *et al*, 2004, 2006; Ginovart *et al*, 2006).

Although it is generally accepted that competition between D2 radioligands and endogenous DA affects the binding of ligands at D2 receptors, the temporal discrepancy between changes in DA levels and radioligand binding is not fully explained by the competition model. Following intravenous amphetamine administration, the increase in extracellular DA and behavioral activation lasts about 2 h (Ichikawa and Meltzer, 1992; Laruelle *et al*, 1997b), whereas the *in vivo* decrease in D2 receptor BP measured with PET or SPECT ligands lasts about 4 to 24 h (Laruelle *et al*, 1997b; Carson *et al*, 2001; Narendran *et al*, 2007). G-protein-coupled receptors (GPCRs), including D2 receptors, show agonist-induced internalization (Ito *et al*, 1999; Vickery and von Zastrow, 1999; Macey *et al*, 2004; Paspalas *et al*, 2006), which might account for the temporal discrepancy (Laruelle, 2000).

Like most GPCRs, D2 receptor internalization is regulated by GPCR kinases (GRKs) and arrestins (Ito *et al*, 1999; Kim *et al*, 2001; Macey *et al*, 2004; Heusler *et al*, 2008; Namkung *et al*, 2009), which target the receptor to clathrin-coated pits for internalization (Tsao *et al*, 2001; Perry and Lefkowitz, 2002). Agonist-induced internalization of D2 receptors would result in a reduction in BP if the B_{max} or K_D of the receptors for the ligands was reduced by internalization, which might be due to diminished ligand access or to changes in receptor conformation in the microenvironment associated with internalization.

To address the role of D2 receptor internalization in the readout of neuroimaging ligands, we developed an *in vitro* system to measure binding to surface and internalized D2 receptors independently. Human embryonic kidney 293 (HEK293) cells were stably transfected with D2 receptors (Javitch *et al*, 2000) tagged with enhanced yellow-fluorescent protein (EYFP), and co-transfected with GRK2 and arrestin 3 to foster robust D2 receptor internalization. We demonstrate that these cells show robust D2 receptor internalization, allowing us to address the effect of receptor internalization on the binding of the most-used neuroimaging ligands.

MATERIALS AND METHODS

Cell System

T-REx-293 cells, a Tetracycline-Regulated Expression cell line (Invitrogen, Carlsbad, CA, USA), were grown in Dulbecco's modified Eagle's medium (GIBCO) containing 10% fetal calf serum and 5 μg/ml blasticidin at 37°C with 5% CO_2, and passaged weekly. The bovine GRK2 and rat arrestin 3 cDNAs were subcloned into T-REx expression plasmids pcDNA4/TO and pcDNA5/TO (Invitrogen), respectively, and confirmed by sequencing. The human short isoform of D2 receptor (D2S) cDNA with a FLAG epitope at the amino terminus was fused with EYFP at the carboxyl terminus and subcloned into the bicistronic expression vector pCIN4 (Rees *et al*, 1996; Javitch *et al*, 2000). The constructs pcDNA4-GRK2 and pcDNA5-arrestin 3 were serially co-transfected into the T-Rex-293 cells using lipofectamine (Invitrogen). Zeocin- and hygromycin-resistant cells were selected. GRK2 and arrestin 3 expression was examined by immunoblotting following tetracycline induction (see below). The construct pCIN4-D2S was then transfected into the stable doubly transfected cells, and the triple-transfected cells were selected in the presence of 700 μg/ml G418, in addition to hygromycin, Zeocin, and blasticidin.

Western Blot Analysis

Control T-REx-293 and the triple-transfected cells were treated with tetracycline or vehicle for 24 h, and then solubilized with 1% dodecyl maltopyranoside in phosphate-buffered saline (PBS) buffer (11 mM Na_2HPO_4, 154 mM NaCl, 2.7 mM KCl, 1 mM $MgCl_2$, 0.1 mM $CaCl_2$, 2 μg/ml pefabloc, 2 μg/ml aprotinin, 1 μg/ml leupeptin, 1 μg/ml pepstatin A, and 10 mM *N*-ethylmaleimide). Protein lysates (20 μg) were separated by SDS-PAGE using a 7.5% polyacrylamide gel and transferred to a polyvinylidene difluoride (PVDF) membrane (Millipore, Bedford, MA). Membranes were blocked for 30 min at room temperature with 5% nonfat milk, 1% bovine serum albumin (BSA), 0.1% Tween 20 in Tris-buffered saline (TBST; 50 mM Tris–HCl, 150 mM NaCl, pH 7.4). Primary antibodies, anti-GRK2 rabbit polyclonal (1 : 1000, Santa Cruz Biotechnology), anti-arrestin 3 rabbit polyclonal (1 : 500, Sigma-Aldrich), and anti-FLAG rabbit polyclonal (1 : 10 000, Sigma-Aldrich) were incubated with the PVDF membranes at room temperature for 1 h to detect GRK2, arrestin 3, and D2 receptor, respectively. Membranes were then washed three times for 10 min each with TBST, incubated with horseradish peroxidase-conjugated anti-rabbit-antibody (1 : 15 000, Santa Cruz Biotechnology) at room temperature for 1 h, and washed three times. Immunoblots were treated with ECL-Plus reagent (Amersham Biosciences, Piscataway, NJ); proteins were visualized and quantitated on a FluorChem 8000 (Alpha Innotech Corporation, San Leandro, CA).

Drug Treatment

Tetracycline. Triple-transfected cells were grown in 100-mm culture dishes for 3–5 days until they were 80–90% confluent. To induce expression of GRK2 and arrestin 3, tetracycline was added to the cells (T+) at a final concentration of 1 μg/ml for 24 h at 36°C. Control cells (T−) were incubated with the same volume of vehicle solution.

Quinpirole. To induce D2 receptor internalization, tetracycline-treated (T+) and control (T−) cells were incubated

with quinpirole (T+/Q+; T−/Q+) at a final concentration of 30 μM for 3 h at 36°C. Control cells (T+/Q−, T−/Q−) were incubated with vehicle. After quinpirole treatment, the medium was removed and the cells were washed with 10 ml PBS (pH 7.4) at 4°C and used in the immunolabeling or radioligand-binding procedures as described. As neither tetracycline alone nor basal expression of GRK2 and arrestin 3 affected D2R internalization, all radioligand binding studies were carried out on tetracycline-treated cells.

MTSET. The sulfhydryl-specific reagent [2-(trimethylammonium)ethyl] methanethiosulfonate bromide (MTSET) is a membrane-impermeant, positively charged polar molecule that reacts with the sulfhydryl group of Cys114 in the binding-site crevice of the D2 receptor to inhibit ligand binding (Javitch *et al*, 1994, 2000). MTSET was used to inactivate cell surface D2 receptors selectively. Aliquots of control and quinpirole-treated cell suspensions (100 μl) were incubated with freshly dissolved MTSET at final concentrations of 0.03–10 mM at 4°C for 15 min. In competition and saturation binding studies, cells were incubated with 5 mM MTSET. The reaction was slowed by addition of cold binding buffer to the cell suspensions to a final volume of 500 μl (see below).

Immunohistochemistry and Flow Cytometry Quantification

To visualize internalization, cells were washed three times with ice-cold HEPES saline buffer (25 mM HEPES, 140 mM NaCl, 5.4 mM KCl, 10% goat serum, pH 7.4). An anti-FLAG labeling mixture was prepared by adding 5 μg Zenon-Alexa 647 mouse IgG labeling reagent A (Invitrogen) to 0.4 μg anti-FLAG antibody in 15 μl PBS (without Ca^{2+} and Mg^{2+}) at room temperature for 5 min, then adding 5 μg IgG labeling reagent B, and incubating for 5 min, adjusting the total volume to 100 μl by adding 10% goat serum in HEPES-buffered saline. For fluorescence microscopic imaging, we applied the labeling mixture to cells grown in microwell dishes (MatTek, Ashland, MA) and incubated for 40 min at 4°C. Cells were washed with HEPES-buffered saline three times, and viewed using an Axiovert 35M (Zeiss). Digital images were captured (Photometrics Sensys camera, Roper Scientific, Tucson, AZ) with iVision software (BioVision, Exton, PA). Sequential imaging was carried out using a diamond objective scriber to mark the regions of interest. Zenon-fluorescence labeling identified surface D2 receptors, and EYFP labeling identified both surface and internalized receptors.

For flow cytometry, dissociated cells were incubated under the same conditions. Surface receptors were labeled using the transfected D2 receptor N-terminal FLAG-tag with anti-FLAG-mouse and anti-mouse-PE antibodies (Invitrogen) diluted 1 : 500 in PBS (with 0.1% of BSA and 0.1% of NaN_3), and quantitated using a Guava EasyCyte (Millipore).

Radioligand Binding

Whole-cell suspension. Cells were dissociated by gentle trituration in 3 ml of binding buffer (25 mM HEPES, 140 mM NaCl, 5.4 mM KCl, 0.006% BSA, 1 mM EDTA, pH 7.4) at 4°C, counted with a hemocytometer, and diluted with cold binding buffer to make the cell suspension of 1.9×10^6–2.8×10^6 cells/ml. To reduce oxidation of DA and D2 agonists in competition binding assays, 0.1% ascorbic acid was added to the binding buffer.

Competition binding. To determine whether [^{3}H]*N*-methylspiperone (NMSP) and [^{3}H]raclopride bound to both surface and internalized D2 receptors, sulpiride, a D2 antagonist with a fixed negative charge, was used as a competitor at surface receptors. Intact cells (100 μl of cell suspension) were incubated with 100 μl of sulpiride at final concentrations of 10^{-13}–10^{-3} M and 100 μl of radioligand [^{3}H]NMSP (0.3 ± 0.1 nM) or [^{3}H]raclopride (1.5 ± 0.5 nM), respectively. To measure ligand affinity for surface and internalized receptors, competition studies were carried out in a minimum of 6 independent experiments under control (Q−/MTSET−) and internalization (Q+/MTSET+) conditions using [^{3}H]raclopride (1.5 nM) and competitors, including the imaging agents (raclopride, IBZM, NMSP, fallypride, FLB 457, epidepride, PHNO and NPA) and control agents (quinpirole, dopamine and sulpiride). Nonspecific binding was determined in the presence of 10 μM (+)-butaclamol. Each binding experiment was carried out in duplicate, and the reaction mixtures (final volume 500 μl) were vortexed and then incubated at 4°C for 3.5 h. The incubation was terminated by rapid filtration on a Cell Harvester (Brandel, Gaithersburg, MD) through GF/B filters pretreated with 0.3% polyethyleneimine. The filters were washed four times with ice-cold Tris–HCl buffer (10 mM Tris–HCl, 120 mM NaCl, pH 7.4), and the radioactivity on the filters was counted with a scintillation counter (Packard, Meriden, CT). The competition curves were analyzed by comparison of two-site *vs* one-site binding models with nonlinear curve fitting (Prism 4, GraphPad Software, San Diego, CA).

Saturation binding. Following MTSET treatment, which blocks binding of ligands to surface D2 receptors, cells (100 μl) were incubated with six concentrations of [^{3}H]NMSP (0.008–0.6 nM) or [^{3}H]raclopride (0.25–6.0 nM) in a final volume of 500 μl. Specific binding was defined as the total binding minus the nonspecific binding obtained in the presence of 10 μM (+)-butaclamol. The binding was carried out in duplicate at 4°C for 3.5 h and terminated by rapid filtration on the Cell Harvester. The K_D and B_{max} values were determined by curve fitting (Prism 4).

RESULTS

Tetracycline-Induced GRK2 and Arrestin 3 Expression

T-REx-293 cells stably expressing D2-EYFP receptors were engineered for tetracycline-induced expression of GRK2 and arrestin 3 to facilitate robust agonist-induced D2 receptor internalization. Both control T-REx-293 and triple-transfected cells showed low basal expression of GRK2 and arrestin 3 (Figure 1a). Tetracycline increased GRK2 and arrestin 3 expression dramatically, with 190 ± 24% increases in GRK2 ($n = 3$) and 538 ± 75% in arrestin 3 ($n = 2$) expression in the triple-transfected cells, compared with untreated cells.

Visualization of D2 Receptor Internalization

Monolayers of triple-transfected cells were examined when they were close to confluence (Figure 1b1). The enhancement of GRK2 and arrestin 3 expression resulted in robust agonist-induced D2 receptor internalization. Under control conditions (without tetracycline or quinpirole, or tetracycline alone, D2 receptors were mainly expressed on the cell surface, as indicated by the surface fluorescence of EYFP-tagged D2 receptors (Q−, Figure 1b2). Following tetracycline induction and quinpirole treatment, EYFP-labeled receptors shifted to the cytoplasm, forming a characteristic punctate endocytic distribution (Q+, Figure 1b3). As neither tetracycline nor quinpirole alone induced D2 receptor internalization, cells were pretreated with tetracycline in all subsequent imaging and binding experiments, and internalization was induced by quinpirole.

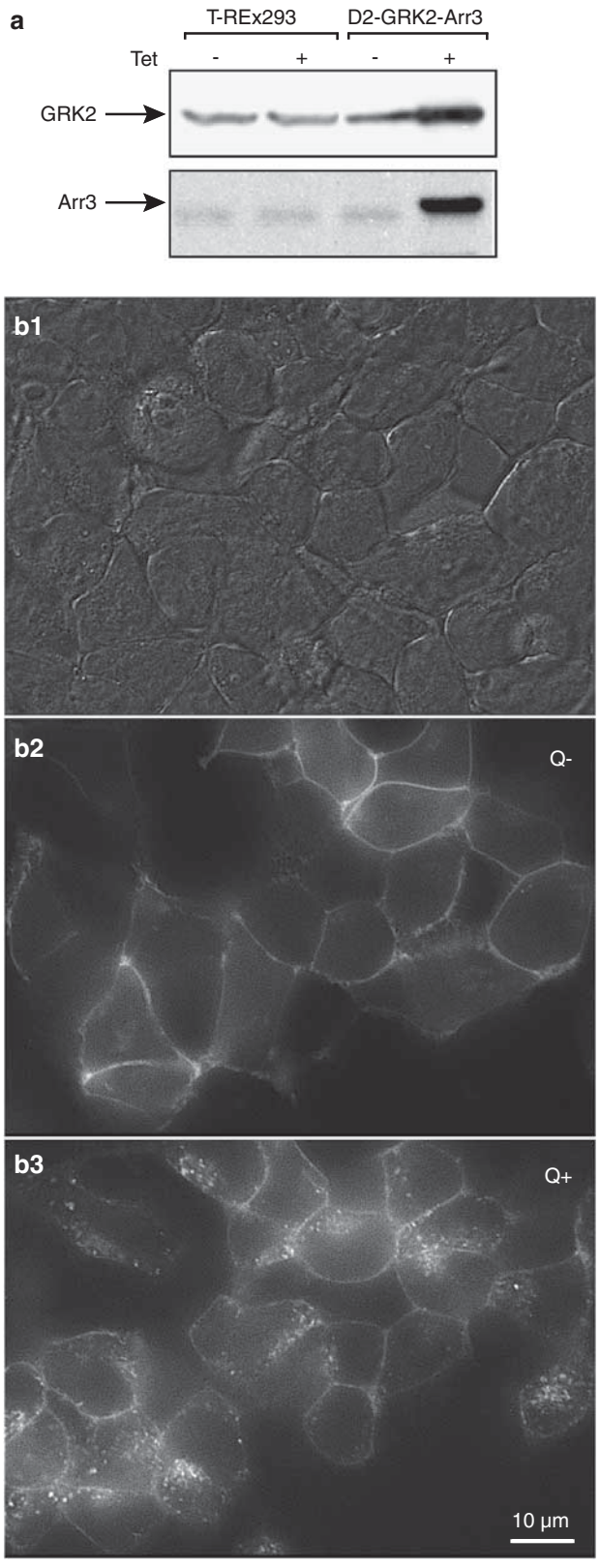

Figure 1 Visualization of GRK2- and arrestin 3-enhanced quinpirole-induced D2 receptor internalization. T-REx-293 cells were triple transfected with D2 receptors, with a FLAG epitope on the extracellular N-terminus and yellow-fluorescent protein (YFP) on the intracellular C-terminus of D2 receptors, GRK2, and arrestin 3 (Arr3). (a) Immunoblot analysis of preparations from T-REx-293 control and D2-GRK2-Arr3 triple-transfected cells. Tetracycline had no effect on the basal expression of GRK2 and arrestin 3 in control T-REx-293 cells (left), while it induced robust expression of GRK2 and arrestin 3 in the triple-transfected cells. GRK2 and arrestin 3 proteins were detected by polyclonal anti-GRK2 and anti-arrestin 3 antibodies, respectively. (b) Cells were treated with tetracycline and then viewed under DIC optics (b1) or epic-fluorescence (b2), and then again following quinpirole treatment (b3). Under control condition (Q−), D2 receptors were mainly expressed at the cell surface, as indicated by the surface fluorescence labeling of Zenon anti-FLAG and D2 receptor-YFP fluorescence (b2). Quinpirole (Q+) induced a dramatic redistribution of EYFP fluorescence into a punctate intracellular pattern, reflecting robust D2 receptor internalization (b3). Cells moved significantly during the quinpirole incubation so the fluorescence images are not directly super imposable.

Quantitation of Internalization with Flow Cytometry

To detect internalization, we used Zenon-labeled anti-FLAG Fab fragments directed to the FLAG epitope on the extracellular D2 receptor N-terminus. Under control conditions, nearly all D2 receptors were located on the surface, as the EYFP fluorescence (visualized in red) and Zenon fluorescence (visualized in green) overlapped (appearing yellow), outlining the plasma membrane (Figure 2a1). Following quinpirole treatment, surface labeling diminished (less yellow), and many receptors were internalized, appearing in a punctate intracellular pattern (red) (Figure 2a2). We used flow cytometry to quantify internalization by analyzing anti-FLAG labeling of surface receptors (Figure 2b). An example of the distribution of fluorescence intensity for surface D2 receptors before (black) and after (red) quinpirole administration is shown in Figure 2b1. Time-course studies revealed maximal D2 receptor internalization of about 58% following quinpirole treatment with a $t_{1/2}$ of about 5 min (Figure 2b2).

Internalization Quantification with [^{3}H]NMSP and [^{3}H]Raclopride Binding

[^{3}H]NMSP binding. To measure binding to internalized D2 receptors in intact cells, we treated cells with quinpirole, inactivated the remaining surface receptors with MTSET, and carried out binding using the lipophilic ligand [^{3}H]NMSP. Consistent with the fluorescence imaging data,

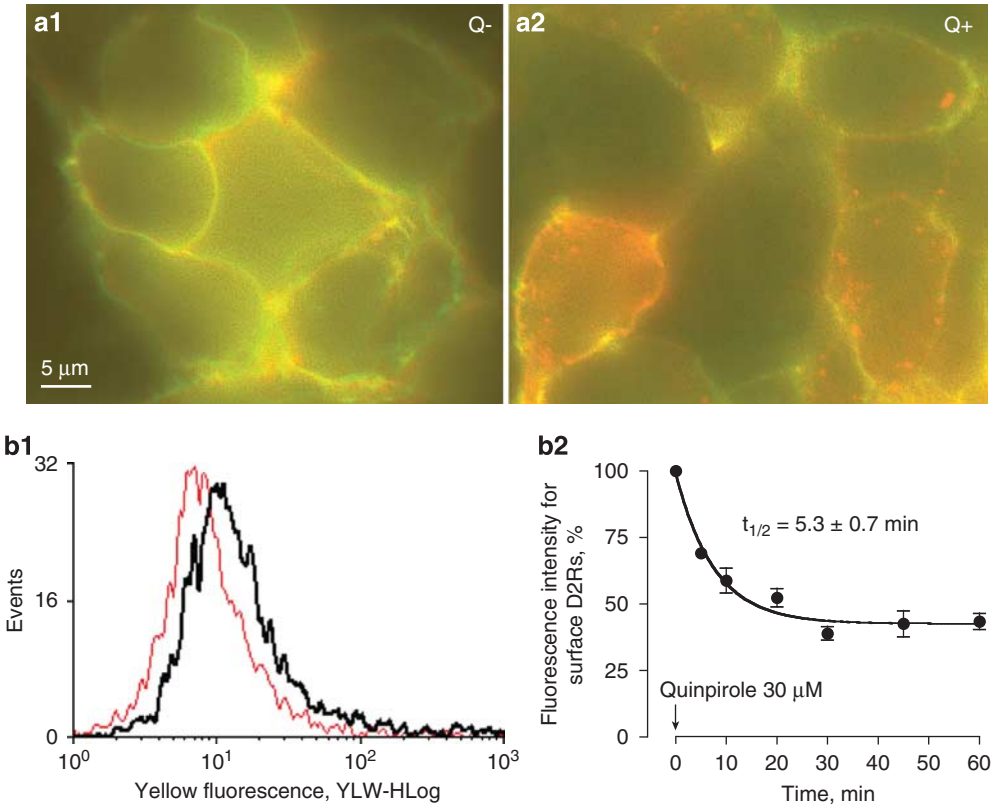

Figure 2 Fluorescence imaging and quantification of quinpirole-induced D2 receptor internalization. (a1) Surface D2 receptors were visualized with Zenon anti-FLAG Fab fragments directed to the FLAG epitope on the extracellular N-terminus (digitized to green) and the EYFP fluorescence of the EYFP tag on the D2 receptor C-terminus (digitized to red) in control cells (Q−). The overlap in the labeling appears yellow in the color merge shown. (a2) Following quinpirole treatment (Q+), internalized D2 receptors show solely EYFP fluorescence (red). (b1) Quinpirole-induced D2 receptor internalization was quantitated using flow cytometry. The histogram shows the distribution of fluorescence intensity for surface D2 receptors before (black) and after (red) quinpirole treatment. (b2) Time-course studies ($n = 3$; time constant as indicated) revealed that after quinpirole treatment, about 42% D2 receptors remained on the surface, implying that about 58% underwent internalization.

[^{3}H]NMSP binding showed that most D2 receptors were susceptible to inactivation by membrane-impermeant MTSET under baseline conditions, and therefore on the surface. [^{3}H]NMSP binding in control cells (Q−) dropped to 10% of the total binding in the presence of MTSET (3–10 mM; Figure 3a), indicating that under control conditions, about 90% of receptors were on the cell surface. After quinpirole treatment (Q+), MTSET inactivated only about 50% of [^{3}H]NMSP binding (Figure 3a), indicating that about 40% of D2 receptors underwent internalization, and were thus protected from MTSET inactivation.

Sulpiride competition with [^{3}H]NMSP revealed a two-site binding curve under control conditions (Q−), with the majority of D2 receptors showing a high affinity (89.9%, Ki = 9.1 ± 1.0 nM) and the minority showing a very low affinity (10.1%, Ki = 142.5 ± 26.8 μM, Figure 3b). Because sulpiride is relatively impermeant due to its fixed negative charge (Mizuchi *et al*, 1983; Honda *et al*, 1977), the high-affinity sites presumably correspond to surface D2 receptors ($Ki_{(s)}$) and the low-affinity sites to internalized D2 receptors ($Ki_{(i)}$). Following quinpirole treatment (Q+), 55% of D2 receptors retained high affinity ($Ki_{(s)} = 9.4 \pm 2.6$ nM), whereas 45% showed low affinity ($Ki_{(i)} = 142.9 \pm 26.3$ μM), indicating that about 35% of receptors underwent internalization (Figure 3b).

[^{3}H]raclopride binding and raclopride competition. Due to its lower lipophilicity compared with NMSP, raclopride was expected to have more limited access to internalized D2 receptors (Laruelle, 2000). To test this, we examined the binding of [^{3}H]raclopride using the same binding paradigm we established for [^{3}H]NMSP, with both sulpiride and raclopride as competitors. Similar to [^{3}H]NMSP binding, MTSET at concentrations of ⩾3 mM inactivated 90% of [^{3}H]raclopride binding in control cells (Q–), but only about 50% in quinpirole-treated cells (Q+) (data not shown). [^{3}H]Raclopride binding in competition with sulpiride also revealed a two-site binding curve, with a $Ki_{(s)} = 7.7 \pm 2.3$ nM for surface D2 receptors (85.8%) and a $Ki_{(i)} = 141.8 \pm 45.2$ μM for intracellular D2 receptors (14.2%) in control cells (Q−). Following quinpirole treatment (Q+), 43.1% of D2 receptors remained on the cell surface ($Ki_{(s)} = 7.9 \pm 3.0$ nM) and 56.9% were inside ($Ki_{(i)} = 120.7 \pm 35.8$ μM), showing that about 43% of D2 receptors underwent internalization (Figure 4a).

The similarity between [^{3}H]NMSP and [^{3}H]raclopride binding in competition with sulpiride suggested that [^{3}H]raclopride bound to internalized receptors in a manner qualitatively similar to that of [^{3}H]NMSP. In contrast to sulpiride, raclopride competition binding with [^{3}H]NMSP (Figure 4b) showed an overlap of one-site binding curves in control (Q−, Ki = 0.26 ± 0.09 nM) and quinpirole-treated

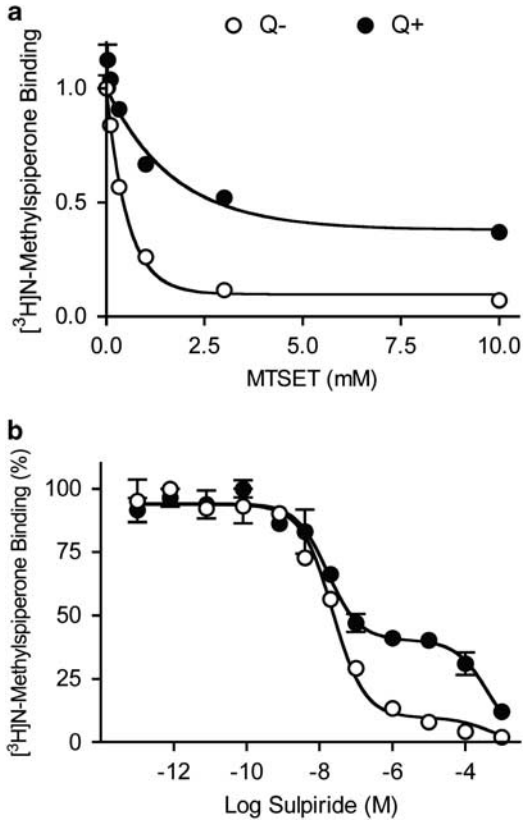

Figure 3 Effect of MTSET and competition with sulpiride on [^{3}H]NMSP binding. Binding assays were carried out in intact cells using [^{3}H]NMSP and quinpirole to induce internalization. (a) Surface receptors were inactivated with increasing concentrations of MTSET. Under control conditions (○, Q−), MTSET inactivated 90% of [^{3}H]NMSP binding. After quinpirole treatment (●, Q+), MTSET inactivated only about 55% of [^{3}H]NMSP binding, indicating that about 45% of D2 receptor underwent internalization. (b) Surface receptors were blocked with the relatively membrane-impermeant antagonist sulpiride. Under control conditions (○, Q−), sulpiride competition binding showed a two-site [^{3}H]NMSP binding curve; the majority of D2 receptors (90%) were accessible to sulpiride and thus subject to competition at high affinity ($Ki_{(s)} = 9.1 \pm 1.0$ nM), whereas only a small minority (10%), presumably internalized, were relatively inaccessible and hence subject to competition at low affinity ($Ki_{(i)} = 142.5 \pm 26.8$ μM). Following quinpirole treatment (●, Q+), the high-affinity [^{3}H]NMSP binding was reduced to 55%, whereas the low-affinity binding increased to about 45%, consistent with robust D2 receptor internalization.

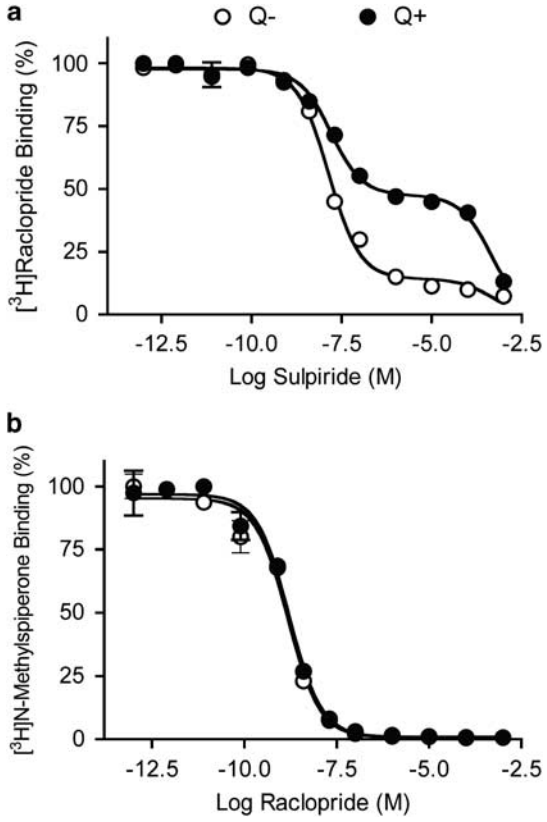

Figure 4 Competition binding of [^{3}H]raclopride or [^{3}H]NMSP under control and internalization conditions. (a) [^{3}H]Raclopride binding in competition with sulpiride. A two-site binding curve was observed in control cells (○, Q−). Most D2 receptors (85.8%) were on the surface and showed high affinity ($Ki_{(s)} = 7.7 \pm 2.3$ nM). A small proportion (14.2%) were internalized and showed low-affinity binding ($Ki_{(i)} = 141.8 \pm 45.2$ μM). Following quinpirole treatment (●, Q+), 43.1% of D2 receptors remained on the surface ($Ki_{(s)} = 7.9 \pm 3.0$ nM) and 56.9% were internalized ($Ki_{(i)} = 120.7 \pm 35.8$ μM). (b) [^{3}H]NMSP binding in competition with raclopride. Competition experiments showed indistinguishable one-site binding curves between control (○, Q−; $Ki = 0.26 \pm 0.09$ nM) and quinpirole-treated cells (●, Q+; $Ki = 0.28 \pm 0.05$ nM). Thus, similar to NMSP, raclopride readily accesses internalized D2 receptors.

cells (Q+, $Ki = 0.28 \pm 0.05$ nM), confirming that raclopride binds to both surface and internalized D2 receptors.

Impact of Internalization on Ligand Affinity

The experiments described above showed that most D2 receptors are at the cell surface under basal conditions, whereas about 40% of D2 receptors are internalized following quinpirole treatment, and that [^{3}H]NMSP and [^{3}H]raclopride bind to both the surface and internalized D2 receptors. As MTSET inactivated nearly all binding under control conditions, untreated cells (Q−/MTSET−) could be used to measure binding to surface receptors. Following agonist and MTSET treatments, receptors remaining on the cell surface were inactivated so treated cells (Q+/MTSET+) could be used to measure binding to internalized receptors. Thus, these two conditions provided independent means to measure the affinity of surface and internalized D2 receptors with different neuroimaging ligands in saturation and competition studies.

Saturation binding. Under control conditions (Q−/MTSET−), [^{3}H]NMSP binding showed a K_D value of 0.12 ± 0.02 nM and a B_{max} value of 37.75 pmol per 10^5 cells (Figure 5a). Saturation binding at internalized receptors (Q+/MSET+) indicated a significant ($p < 0.01$, $n = 3$) increase in the [^{3}H]NMSP K_D (0.48 ± 0.13 nM), suggesting a significant decrease in affinity. As expected, the B_{max} decreased (19.35 pmol per 10^5 cells) ($p < 0.01$, $n = 3$) because of MTSET inactivation of surface receptors following quinpirole treatment, indicating that about 51% of D2 receptors had undergone internalization. Confirming its accessibility to internalized D2 receptors, [^{3}H]raclopride saturation binding also showed a small but significant increase in K_D in quinpirole-treated cells (Q+/MTSET+:

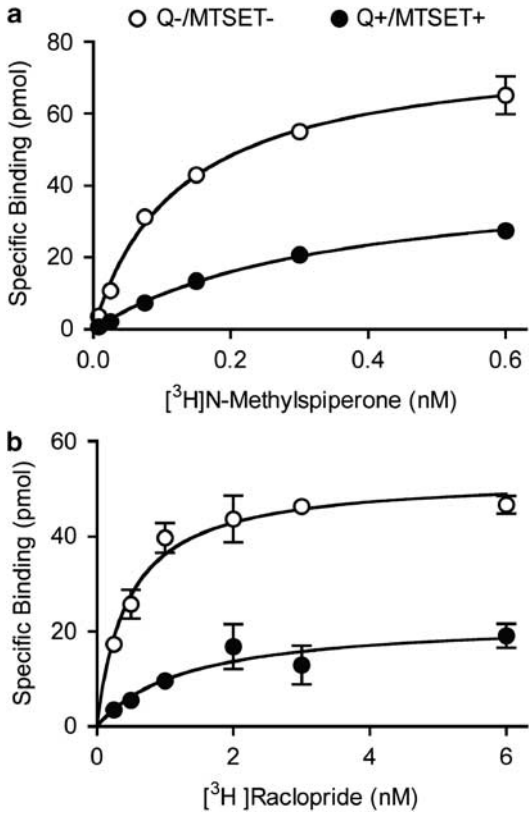

Figure 5 Saturation binding to surface and internalized D2 receptors. (a) Under control conditions, when most receptors are on the surface, [^{3}H]NMSP saturation binding showed a one-site binding curve with a K_D of 0.12 ± 0.02 nM (○, Q−/MTSET−). Following quinpirole and inactivation of surface receptors with MTSET, the remaining functional internalized D2 receptors showed a one-site binding curve with a lower-affinity K_D of 0.48 ± 0.13 nM (●, Q + /MTSET +). On the basis of the reduction in the B_{max}, ~50% of D2 receptors underwent internalization. (b) Under control conditions, [^{3}H]raclopride saturation binding showed a K_D of 0.5 ± 0.1 nM. Following quinpirole and MTSET, binding showed a lower-affinity K_D of 1.2 ± 0.2 nM. On the basis of the reduction in B_{max} with raclopride binding, ~40% of D2 receptors underwent internalization.

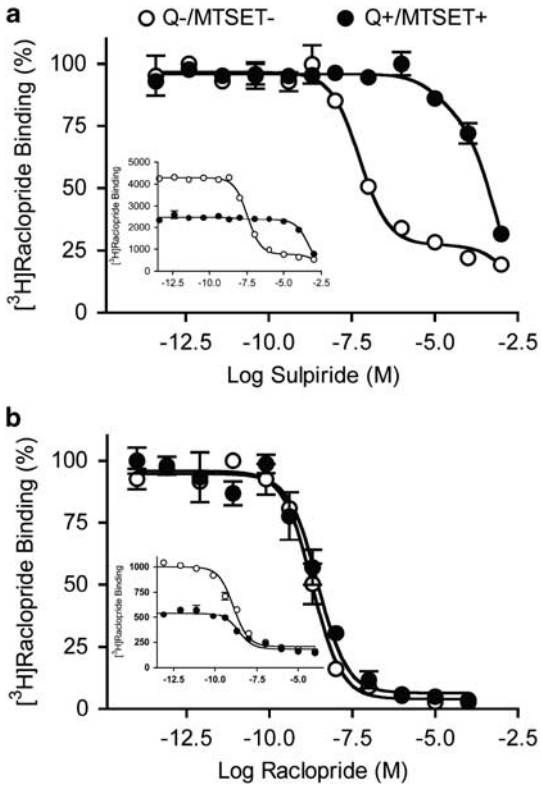

Figure 6 Sulpiride and raclopride competition binding with [^{3}H]raclopride in MTSET-treated cells. (a) Competition with sulpiride showed two different binding curves under control and internalization conditions. A two-site [^{3}H]raclopride binding curve showed that the majority (80.9%) of D2 receptors were on the surface ($Ki_{(s)}$ = 10.3 ± 12.3 nM) in control (○, Q−/MTSET−), and a one-site binding curve indicated the poor accessibility ($Ki_{(i)}$ = 206.0 ± 23.6 μM) of sulpiride to internalized D2 receptors in treated cells (●, Q + /MTSET +). (b) In contrast, raclopride competition binding showed similar one-site binding curves under both control and internalization conditions, with about twofold increases in the Ki value as indicated by the right-shift of the binding curve in treated cells (●) compared with control (○). The insets show the same binding data, but plotted without normalizing the binding parameters, to allow for quantitative comparison of binding in control and treated cells.

$K_D = 1.2 \pm 0.2$ nM, $p < 0.001$, $n = 6$) compared with the control cells (Q−/MTSET−: $K_D = 0.5 \pm 0.1$ nM) and a significant reduction in B_{max} (Q−/MTSET−: $B_{max} = 22.68$ pmol per 10^5 cells, Q + /MTSET + : $B_{max} = 8.8$ pmol per 10^5 cells; Figure 5b), indicating that about 39% of D2 receptors underwent internalization.

Competition with D2 antagonists and agonists. Using [^{3}H]raclopride as the radioligand, competition binding was carried out to examine the accessibility of different D2 antagonist and agonist imaging ligands and control agents to internalized D2 receptors in treated (Q + /MTSET +) *vs* control cells (Q−/MTSET−). Antagonist competition curve fits are shown in Figure 6, and Supplementary Figure S1 (in the Supplementary Information), and agonist competition curve fits are shown in Supplementary Figure S2 (Supplementary Information). As expected, a large decrease in potency to block [^{3}H]raclopride binding to internalized receptors was observed for sulpiride, indicating the poor accessibility of sulpiride to internalized D2 receptors (Figure 6a; Table 1). In contrast, competition with raclopride showed similar one-site binding curves under both control and internalization/surface D2R-inactivation conditions (Figure 6b).

Consistent with the saturation binding, raclopride competition also showed a small but significant increase in Ki value in MTSET-treated cells following quinpirole (Figure 6b; Table 1). Similarly, all tested antagonist imaging ligands (Supplementary Figure S1, Supplementary Information) were able to compete at internalized receptors with high affinity. A small but significant increase in the Ki value for quinpirole plus MTSET-treated cells was observed in competition with NMSP (Table 1; Supplementary Figure S1B), fallypride (Table 1; Supplementary Figure S1C), FLB 457 (Table 1; Supplementary Figure S1D), and epidepride (Table 1; Supplementary Figure S1E). In agonist competition studies, only a modest change in potency to inhibit [^{3}H]raclopride binding to internalized receptors was observed for the imaging agents PHNO (Table 1; Supplementary Figure S2B), but not NPA nor the control agent quinpirole (Table 1; Supplementary Figure SA2, S2C); all were able to compete at internalized receptors with high affinity. In contrast, DA

Table 1 Effect of Internalization on the Affinity of Commonly Used Neuroimaging Agents

Type of ligand	Pharmacology	Ligand (number of experiments)	Surface D2 receptor (Q−/MTSET−) ($Ki_{(s)}$, nM)	Internalized D2 receptor (Q+/MTSET+) ($Ki_{(i)}$, nM)	Affinity shift ($Ki_{(i)}/Ki_{(s)}$)	Lipophilicity (Log P[†] or Log kw[‡])
Imaging	Antagonist	Raclopride (6)	0.50 ± 0.08	1.00 ± 0.35*	2.1	1.3[†] (Laruelle, 2000)
		FLB 457 (5)	0.03 ± 0.01	0.09 ± 0.02**	3.0	1.9[‡] (Loc'h *et al*, 1996)
		Epidepride (6)	0.01 ± 0.01	0.03 ± 0.01*	2.4	2.1[‡] (Kessler *et al*, 1991)
		Fallypride (6)	0.32 ± 0.06	0.92 ± 0.31**	2.9	2.4[†] (Laruelle, 2000)
		IBZM (9)	0.19 ± 0.05	0.23 ± 0.11	1.2	2.8[†] (Laruelle, 2000)
		NMSP (6)	0.07 ± 0.01	0.13 ± 0.02**	1.9	3.3[†] (Laruelle, 2000)
	Agonist	PHNO (9)	2.62 ± 0.56	5.67 ± 2.90*	2.2	2.1[†] (Wilson *et al*, 2005)
		NPA (6)	0.97 ± 0.28	1.02 ± 0.33	1.1	2.5[†] (Wilson *et al*, 2005)
Control	Agonist	Dopamine (6)	870.3 ± 146	19,337 ± 4265**	22.2,	0.6[a,†]
		Quinpirole (7)	900.4 ± 138.3	856.1 ± 120.5	1.0	2.4[a,†]
	Antagonist	Sulpiride (3)	10.3 ± 2.3	202,000 ± 25,300**	19,600	1.3[†] (de Paulis *et al*, 1988)

[a]Calculated with Chemdraw Ultra 11.0.1 (CambridgeSoft, Cambridge, MA).
*$p<0.01$ *vs* $Ki_{(s)}$; **$p<0.001$ *vs* $Ki_{(s)}$, *t*-test.
Ki values were measured for surface ($Ki_{(s)}$, Q−/MTSET− conditions) and internalized ($Ki_{(i)}$ Q+/MTSET+ conditions) D2 receptors.
Two-way ANOVA restricted to the imaging agents with conditions (Q−/MTSET− *vs* Q+/MTSET+) and ligands as factors further revealed a significant effect of conditions ($p=0.003$), ligands ($p<0.001$), and condition by ligand interactions ($p<0.001$).

(Table 1; Supplementary Figure S2D), which similar to sulpiride diffuses poorly into cells, showed a dramatic reduction in binding to internalized receptors.

For the seven imaging agents, a two-way ANOVA on Ki value under the control and internalization/membrane D2R-inactivation conditions (Q−/MTSET− *vs* Q+/MTSET+), with ligands as factors revealed a significant effect of condition ($p=0.003$), ligands ($p<0.001$) and condition by ligands interactions ($p<0.001$). Thus, internalization was associated with a small but significant loss of affinity overall. The magnitude of the effect varied among the ligands tested. *Post hoc* analysis carried out on normalized values revealed that the internalization effect was significantly larger for fallypride and FLB 457, compared with IBZM and NPA, but not significantly different from the other ligands.

DISCUSSION

We examined the impact of D2 receptor internalization on the binding affinities of D2 receptor antagonists and agonists commonly used in PET and SPECT imaging studies. Initial experiments in T-REx-293 cells stably transfected with D2 receptors failed to show reliable agonist-induced D2 receptor internalization. Under baseline and following agonist treatment, >90% of D2 receptors remained on the cell surface. In contrast, cells co-transfected with GRK2 and arrestin 3 showed robust agonist-induced internalization, confirming that GRK2 and arrestin 3 have critical roles in agonist-induced D2 receptor internalization (Ito *et al*, 1999; Kim *et al*, 2001; Macey *et al*, 2004; Heusler *et al*, 2008; Namkung *et al*, 2009). Quantification of agonist-induced internalization in triple-transfected cells yielded consistent results with four independent methods: flow cytometry (58% internalized fraction), MTSET inactivation (40%), saturation binding (35% with ^{3}H-NMSP; 43% with ^{3}H-raclopride), and sulpiride competition (51% with ^{3}H-NMSP; 39% with ^{3}H-raclopride). Thus, in the triple-transfected cells, agonist treatment caused about half of cell surface receptors to undergo internalization.

The ligands [^{3}H]NMSP and [^{3}H]raclopride accessed both surface and internalized receptors. Before agonist treatment, membrane-impermeant MTSET abolished the specific binding of both antagonists, indicating that most receptors were indeed on the cell surface. After agonist treatment, the effect of MTSET was lessened, showing specific binding of both ligands to internalized receptors that MTSET could not access. Similarly, sulpiride inhibited most of the binding of both antagonists with high affinity before agonist treatment; following agonist treatment, high-affinity binding was reduced and low-affinity binding increased, presumably reflecting binding of both radiolabeled antagonists to receptors inside the cells. The ability of [^{3}H]NMSP and [^{3}H]raclopride to diffuse into the cells was not unexpected, as [^{11}C]NMSP and [^{11}C]raclopride readily cross the blood–brain barrier, which entails diffusion across several cell membranes. Thus, internalized D2 receptors retain the conformation required for high-affinity binding of NMSP and raclopride.

This cellular system provided a straightforward way to compare the affinity of unlabeled ligands for surface and internalized receptors. The affinity measured under basal conditions (Q−/MTSET−) was the affinity at surface receptors, whereas the affinity measured after quinpirole exposure and MTSET inactivation (Q+/MTSET+) was the affinity at internalized receptors. Comparing [^{3}H]NMSP and

[^{3}H]raclopride affinity in saturation studies under Q−/MTSET− and Q+/MTSET+ conditions provided a first indication that affinity of these drugs for internalized receptors was reduced. As the calculation of Ki value depends on K_D values, the determination of [^{3}H]raclopride K_D values for surface and internalized receptors was a prerequisite for the competition experiments with the neuroimaging ligands.

[^{3}H]Raclopride competition binding experiments were carried out with a number of imaging ligands under both Q−/MTSET− and Q+/MTSET+ conditions. Affinity values measured in this system were consistent with values reported in the literature. The rank order of affinity values was also consistent with values reported in the literature: PHNO, NPA, and raclopride < IBZM, and fallypride < NMSP < FLB457 and epidepride. Analysis of the competition data revealed a significant effect of receptor internalization on Ki values. Internalization was associated with a small but significant reduction in measured affinity. The magnitude of the affinity change varied among ligands, with fallypride and FLB 457 exhibiting larger affinity shifts than IBZM and NPA.

The average decrease in affinity associated with internalization for all the imaging ligands was 2.1 fold. A change of this magnitude would have a direct impact on neuroimaging results. BP is the measured binding parameter and is inversely proportional to K_D ($BP = B_{max}/K_D$). Assuming, for the sake of argument, that all D2 receptors are on the surface under baseline conditions, and that 50% of receptors are internalized following an amphetamine-induced DA surge, then BP would be reduced by 25%. The magnitude of this decrease is comparable with the BP decrease observed following an amphetamine challenge *in vivo* (Laruelle *et al*, 1997b).

There are several potential caveats that need to be considered in the interpretation of our competition studies. Incomplete washout of quinpirole could have led to a reduction in the apparent affinity determined in saturation binding analysis after internalization, but the similarity between our saturation and competition results suggest that this is not a confound. The free ligand concentration in the vicinity of internalized receptors might be lower than in the extracellular milieu because of the time required for ligands to traverse the plasma and endosomal membranes to reach internalized receptors. The existence of a gradient between extracellular ligand and endosomal ligand concentrations could give rise to an apparent increase in the Ki value measured in the competition experiments. And, difficulties in diffusion into cells evidently do translate into changes in apparent affinity, as exemplified by the sulpiride and DA experiments. However, we carried out our studies under quasi-equilibrium conditions in an attempt to obviate differences in free ligand concentration across the membrane. Regardless, this should not affect the implications for neuroimaging studies in which the extracellular concentration is used as the reference concentration to calculate K_D and BP. Changes in binding affinity revealed here should thus parallel the changes in BP observed in neuroimaging studies.

Overexpression of arrestin 3 could alter the affinity of D2 receptors for some ligands and a difference between arrestin binding to surface and internal receptors could conceivably contribute to our findings. Indeed, arrestin 3 binding to purified β_2-adrenergic receptors substantially increases agonist affinity (>10-fold) (Gurevich *et al*, 1997). However, we did not see a consistent effect on the binding of agonists, which should be affected similarly by receptor affinity state; PHNO showed a reduced affinity for internalized receptors, while NPA and quinpirole were unaffected. Therefore, it seems unlikely that binding of arrestin 3 would impact significantly on the binding affinity in our system.

We measured the changes in affinity of internalized D2 receptors 3–4 h after triggering internalization and at 4°C to prevent receptors from recycling back to the plasma membrane. It is not known how rapidly or how many D2 receptors recycle back to the membrane *in vivo*. In HEK-293 cells, at 37°C, D2 receptors degrade slowly ($t_{1/2} > 7$ h) but recycle rapidly back to the membrane ($t_{1/2} > 30$ min) (Vickery and von Zastrow, 1999). It seems likely that significant numbers of receptors recycle back to the membrane during the course of a neuroimaging experiment. However, this would lessen (rather than magnify) the contribution of internalization to the extent and duration of decreases in BP of radioligands in neuroimaging studies. Finally, it remains possible that the T-REx-293 cells we used do not entirely model the differences in neurons in the receptor microenvironment associated with internalization. This issue will require further studies in neurons.

Constrained by these limitations, the results described in this paper have implications for the interpretation of D2 neuroreceptor imaging studies. We show that all the tested imaging ligands bind with high but different affinity to surface and internalized receptors. The implication is that the specific binding of ligands observed in PET and SPECT imaging studies is a mixture of binding to surface and internalized receptors. As several of the ligands show different affinities for D2 receptors based on internalization status, changes in D2 receptor BP observed in pathological conditions may be due to differences in internalization status. The results generally support the hypothesis that changes in internalization status following interventions that modulate synaptic DA concentrations contribute to changes in observed BP. As addressed in the Introduction, changes in BP persist well beyond acute fluctuations in extracellular DA concentrations, suggesting that mechanisms other than simple binding competition contribute to the sustained BP decrease following a DA surge. Decreased affinity of internalized receptors might be one such mechanism. One way to test this hypothesis would be to correlate the time course of changes in cellular localization of D2 receptors *in vivo* with the time course of changes in BP following a DA surge.

The differences between ligands in the magnitude of the affinity shift associated with internalization status were not related to differences in affinity, lipophilicity, chemical nature, or pharmacological property (agonists *vs* antagonists). Furthermore, they were not directly related to the magnitude of changes in *in vivo* binding following manipulation of DA release. Of the eight ligands used in this study, five are unquestionably satisfactory neuroimaging ligands, namely, [^{11}C]raclopride, [^{123}I]IBZM, [^{18}F]fallypride, [^{11}C]NPA, and [^{11}C]PHNO. A common property of these imaging ligands is that their moderate affinity and kinetic profile enables proper quantification of D2 receptor

BP in the striatum. The antagonists, [^{11}C]raclopride, [^{123}I]IBZM, and [^{18}F]Fallypride, have been shown to be robustly affected by acute changes in synaptic DA, both in animals and humans. Available evidence suggests that the magnitude of BP decrease after amphetamine is similar for three of these imaging ligands, [^{11}C]raclopride, [^{123}I]IBZM, and [^{18}F]fallypride (Laruelle, 2000; Slifstein *et al*, 2004; Mukherjee *et al*, 2005; Riccardi *et al*, 2006; Cropley *et al*, 2008; Narendran *et al*, 2009). The differences in affinity shifts among the three ligands induced by internalization (fallypride > raclopride > IBZM) observed here suggest that the affinity shift is not the only factor contributing to the long lasting BP changes observed in neuroimaging experiments. Changes that would affect the B_{max} in the brain without changing the affinity, such as receptor modification or degradation, might not be captured by these results. Further study will be needed to test these putative factors.

The vulnerability of [^{11}C]NPA to changes in endogenous DA is larger than that of [^{11}C]raclopride, an observation that has been attributed to fact that [^{11}C]NPA, being a full agonist, binds preferentially to D2 receptors in the high-affinity state, a population of receptors expected to be more affected by changes in synaptic DA (Narendran *et al*, 2004). The difference in affinity shift induced by internalization between these ligands (raclopride > NPA) seen in these studies does not jive with the magnitude of BP decrease ([^{11}C]NPA > [^{11}C]raclopride) after amphetamine (Narendran *et al*, 2004). The *in vivo* vulnerability of [^{11}C]PHNO to DA changes is even higher than that of [^{11}C]NPA, because [^{11}C]PHNO shows higher affinity for D3 compared with D2 receptors, and D3 receptors have higher affinity for DA than D2 receptors (Narendran *et al*, 2006; Graff-Guerrero *et al*, 2009; Rabiner *et al*, 2009). In regions such as the dorsal striatum where D2 receptors are responsible for most of the [^{11}C]PHNO (Searle *et al*, in submission), and [^{11}C]NPA binding signals, changes in [11C[PHNO BP induced by amphetamine are of the same magnitude as [^{11}C]NPA (Narendran *et al*, 2006; Rabiner *et al*, 2009). In the experiments reported here, the affinity shift of PHNO was numerically larger than for NPA, an observation inconsistent with internalization alone accounting for the results of the imaging studies.

Interpreting the results for the very-high-affinity antagonists, [^{11}C]NMSP, [^{11}C]FLB457 and [^{123}I]epidepride, is more complex. Proper *in vivo* quantification of D2 receptors BP with these ligands in high D2 receptor density regions such as the striatum is practically impossible due to the protracted time required for these ligands to reach equilibrium and the vulnerability of their uptake to changes in blood flow. Many contradictory studies have thus been reported in the literature; studies with [^{11}C]NMSP or analogs reported increased, decreased, or no change in BP following amphetamine (Leslie and Bennett, 1987; Bischoff *et al*, 1991; Bischoff and Gunst, 1997; Hartvig *et al*, 1997). Two studies with [^{123}I]epidepride suggested no changes in BP following amphetamine (Al-Tikriti *et al*, 1994; Tibbo *et al*, 1997). From a kinetic point of view, [^{11}C]FLB457 is adequate to measure D2 receptor BP in cortical regions, where the concentration of D2 receptors is much lower. Consistent with this, we have found in humans that the BP of [^{11}C]FLB457 is reduced in the cortex following amphetamine (Narendran *et al*, 2009); however, such a change was not found by others (Okauchi *et al*, 2001; Aalto *et al*, 2009). The low signal-to-noise associated with measurement of cortical D2 receptors might explain this discrepancy. Because of the uncertain nature and magnitude of the vulnerability of these ligands to endogenous DA in imaging paradigms, only a limited comparison with these results is possible.

In conclusion, we have developed an *in vitro* system suitable for independent measurements of the affinity of ligands to surface and internalized D2 receptors. Testing of eight commonly used D2 receptor neuroimaging ligands showed that all ligands bind with high affinity to both surface and internalized receptors. Receptor internalization is associated with a small but significant reduction in binding affinity for six of the eight ligands. To the extent that these findings can be extrapolated to the *in vivo* condition, our results suggest that D2 receptor trafficking may affect the signal measured in neuroimaging studies and may have a role in the sequence of events leading to changes in D2 receptor BP following subsequent to fluctuations in synaptic DA concentrations. However, differences in affinity shifts among the ligands suggest that additional factors beyond receptor trafficking are likely to be involved in these long-lasting changes. Further study will be needed to determine the role of receptor trafficking in these responses, as well as to identify and validate other mechanisms.

ACKNOWLEDGEMENTS

We thank Brian K Clinton and Todd J Harris for initial experiments. This work was supported by the NIMH Conte Center on the *Neurobiology of Dopamine in Schizophrenia* MH066171 (ML, SR), NIH grants DA022413 (JAJ), and MH54137 (JAJ) and DA000356 (SR), by NARSAD (NG, RN) GlaxoSmithKline, and the Lieber Center for Schizophrenia Research and Treatment at Columbia University.

DISCLOSURE

Jonathan A Javitch is on the Scientific Advisory Board of HEPTARES therapeutics. Marc Laruelle is an employee of GlaxoSmithKline. Stephen Rayport is a Scientific Consultant to MatTek. The other authors declare no conflict of interest.

REFERENCES

Aalto S, Hirvonen J, Kaasinen V, Hagelberg N, Kajander J, Nagren K *et al* (2009). The effects of d-amphetamine on extrastriatal dopamine D2/D3 receptors: a randomized, double-blind, placebo-controlled PET study with [^{11}C]FLB 457 in healthy subjects. *Eur J Nucl Med Mol Imaging* **36**: 475–483.

Abi-Dargham A, Rodenhiser J, Printz D, Zea-Ponce Y, Gil R, Kegeles LS *et al* (2000). Increased baseline occupancy of D2 receptors by dopamine in schizophrenia. *Proc Natl Acad Sci USA* **97**: 8104–8109.

Al-Tikriti MS, Baldwin RB, Zea-Ponce Y, Sybriska E, Zoghbi S, Laruelle M *et al* (1994). Comparison of three high affinity SPECT radiotracers for the dopamine D_2 receptors. *Nucl Med Biol* **21**: 179–188.

Bischoff S, Gunst F (1997). Distinct binding patterns of [^{3}H]raclopride and [^{3}H]spiperone at dopamine D2 receptors *in vivo* in rat brain. Implications for PET studies. *J Recept Signal Transduct Res* **17**: 419–431.

Bischoff S, Krauss J, Grunenwald C, Gunst F, Heinrich M, Schaub M *et al* (1991). Endogenous dopamine (DA) modulates [^{3}H]spiperone binding *in vivo* in rat brain. *J Recept Res* **11**: 163–175.

Breier A, Su TP, Saunders R, Carson RE, Kolachana BS, de Bartolomeis A *et al* (1997). Schizophrenia is associated with elevated amphetamine-induced synaptic dopamine concentrations: evidence from a novel positron emission tomography method. *Proc Natl Acad Sci USA* **94**: 2569–2574.

Carson RE, Channing MA, Vuong B, Watabe H, Herscovitch P, Eckelman WC (2001). Amphetamine-induced doopamine release: duration of action assessed with [^{11}C]raclopride in anesthetized monkeys. In: Gjedde A (ed). *Physiological Imaging of the Brain with PET*. Academic Press: San Diego. pp 205–209.

Cropley V, Innis R, Nathan P, Brown A, Sangare J, Lerner A *et al* (2008). Small effect of dopamine release and no effect of dopamine depletion on [^{18}F]fallypride binding in healthy humans. *Synapse* **62**: 399–408.

de Paulis T, Janowsky A, Kessler RM, Clanton JA, Smith HE (1988). (S)-N-[(1-ethyl-2-pyrrolidinyl)methyl]-5-[^{125}I]iodo- 2-methoxybenzamide hydrochloride, a new selective radioligand for dopamine D-2 receptors. *J Med Chem* **31**: 2027–2033.

Ginovart N, Galineau L, Willeit M, Mizrahi R, Bloomfield PM, Seeman P *et al* (2006). Binding characteristics and sensitivity to endogenous dopamine of [^{11}C]-(+)-PHNO, a new agonist radiotracer for imaging the high-affinity state of D2 receptors *in vivo* using positron emission tomography. *J Neurochem* **97**: 1089–1103.

Goggi JL, Sardini A, Egerton A, Strange PG, Grasby PM (2007). Agonist-dependent internalization of D2 receptors: imaging quantification by confocal microscopy. *Synapse* **61**: 231–241.

Graff-Guerrero A, Redden L, Abi-Saab W, Katz DA, Houle S, Barsoum P *et al* (2009). Blockade of [^{11}C](+)-PHNO binding in human subjects by the dopamine D_3 receptor antagonist ABT-925. *Int J Neuropsychopharmacol*; e-pub ahead of print 15 Sep 2009, doi:10.1017/S1461145709990642.

Gurevich VV, Pals-Rylaarsdam R, Benovic JL, Hosey MM, Onorato JJ (1997). Agonist-receptor-arrestin, an alternative ternary complex with high agonist affinity. *J Biol Chem* **272**: 28849–28852.

Hartvig P, Torstenson R, Tedroff J, Watanabe Y, Fasth KJ, Bjurling P *et al* (1997). Amphetamine effects on dopamine release and synthesis rate studied in the Rhesus monkey brain by positron emission tomography. *J Neural Transm* **104**: 329–339.

Heusler P, Newmantancredi A, Loock T, Cussac D (2008). Antipsychotics differ in their ability to internalise human dopamine D2S and human serotonin 5-HT1A receptors in HEK293 cells. *Eur J Pharmacol* **581**: 37–46.

Honda F, Satoh Y, Shimomura K, Satoh H, Noguchi H, Uchida S *et al* (1977). Dopamine receptor blocking activity of sulpiride in the central nervous system. *Jpn J Pharmacol* **27**: 397–411.

Ichikawa J, Meltzer HY (1992). The effect of chronic atypical antipsychotic drugs and haloperidol on amphetamine-induced dopamine release *in vivo*. *Brain Res* **574**: 98–104.

Ito K, Haga T, Lameh J, Sadee W (1999). Sequestration of dopamine D2 receptors depends on coexpression of G-protein-coupled receptor kinases 2 or 5. *Eur J Biochem* **260**: 112–119.

Javitch JA, Li X, Kaback J, Karlin A (1994). A cysteine residue in the third membrane-spanning segment of the human D2 dopamine receptor is exposed in the binding-site crevice. *Proc Natl Acad Sci USA* **91**: 10355–10359.

Javitch JA, Shi L, Simpson MM, Chen J, Chiappa V, Visiers I *et al* (2000). The fourth transmembrane segment of the dopamine D2 receptor: accessibility in the binding-site crevice and position in the transmembrane bundle. *Biochemistry* **39**: 12190–12199.

Kegeles LS, Abi-Dargham A, Zea-Ponce Y, Rodenhiser-Hill J, Mann JJ, Van Heertum RL *et al* (2000). Modulation of amphetamine-induced striatal dopamine release by ketamine in humans: implications for schizophrenia. *Biol Psychiatry* **48**: 627–640.

Kessler RM, Ansari MS, de Paulis T, Schmidt DE, Clanton JA, Smith HE *et al* (1991). High affinity dopamine D_2 receptor radioligands. 1. Regional rat brain distribution of iodinated benzamides. *J Nucl Med* **32**: 1593–1600.

Kim KM, Valenzano KJ, Robinson SR, Yao WD, Barak LS, Caron MG (2001). Differential regulation of the dopamine D2 and D3 receptors by G protein-coupled receptor kinases and β-arrestins. *J Biol Chem* **276**: 37409–37414.

Laruelle M (2000). Imaging neurotransmission with *in vivo* binding competition techniques: a critical review. *J Cereb Blood Flow Metab* **20**: 423–451.

Laruelle M, Abi-Dargham A, van Dyck C, Gil R, De Souza C, Erdos J *et al* (1996). Single photon emission computerized tomography imaging of amphetamine-induced dopamine release in drug free schizophrenic subjects. *Proc Natl Acad Sci USA* **93**: 9235–9240.

Laruelle M, D'Souza CD, Baldwin RM, Abi-Dargham A, Kanes SJ, Fingado CL *et al* (1997a). Imaging D2 receptor occupancy by endogenous dopamine in humans. *Neuropsychopharmacology* **17**: 162–174.

Laruelle M, Iyer RN, al-Tikriti MS, Zea-Ponce Y, Malison R, Zoghbi SS *et al* (1997b). Microdialysis and SPECT measurements of amphetamine-induced dopamine release in nonhuman primates. *Synapse* **25**: 1–14.

Leslie CA, Bennett Jr JP (1987). Striatal D1- and D2-dopamine receptor sites are separately detectable *in vivo*. *Brain Res* **415**: 90–97.

Loc'h C, Halldin C, Bottlaender M, Swahn CG, Moresco RM, Maziere M *et al* (1996). Preparation of [^{76}Br]FLB 457 and [^{76}Br]FLB 463 for examination of striatal and extrastriatal dopamine D-2 receptors with PET. *Nucl Med Biol* **23**: 813–819.

Macey TA, Gurevich VV, Neve KA (2004). Preferential Interaction between the dopamine D2 receptor and Arrestin2 in neostriatal neurons. *Mol Pharmacol* **66**: 1635–1642.

Martinez D, Narendran R, Foltin RW, Slifstein M, Hwang DR, Broft A *et al* (2007). Amphetamine-induced dopamine release: markedly blunted in cocaine dependence and predictive of the choice to self-administer cocaine. *Am J Psychiatry* **164**: 622–629.

Mizuchi A, Kitagawa N, Miyachi Y (1983). Regional distribution of sultopride and sulpiride in rat brain measured by radioimmunoassay. *Psychopharmacology (Berl)* **81**: 195–198.

Mukherjee J, Christian BT, Narayanan TK, Shi B, Collins D (2005). Measurement of d-amphetamine-induced effects on the binding of dopamine D-2/D-3 receptor radioligand, ^{18}F-fallypride in extrastriatal brain regions in non-human primates using PET. *Brain Res* **1032**: 77–84.

Namkung Y, Dipace C, Javitch JA, Sibley DR (2009). G protein-coupled receptor kinase-mediated phosphorylation regulates post-endocytic trafficking of the D2 dopamine receptor. *J Biol Chem* **284**: 15038–15051.

Narendran R, Frankle WG, Mason NS, Rabiner EA, Gunn RN, Searle GE *et al* (2009). Positron emission tomography imaging of amphetamine-induced dopamine release in the human cortex: a comparative evaluation of the high affinity dopamine D2/3 radiotracers [^{11}C]FLB 457 and [^{11}C]fallypride. *Synapse* **63**: 447–461.

Narendran R, Hwang DR, Slifstein M, Talbot PS, Erritzoe D, Huang Y *et al* (2004). *In vivo* vulnerability to competition by endogenous dopamine: comparison of the D2 receptor agonist radiotracer (−)-N-[^{11}C]propyl-norapomorphine ([^{11}C]NPA) with the D2 receptor antagonist radiotracer [^{11}C]-raclopride. *Synapse* **52**: 188–208.

Narendran R, Slifstein M, Guillin O, Hwang Y, Hwang DR, Scher E *et al* (2006). Dopamine (D2/3) receptor agonist positron emission tomography radiotracer [^{11}C]-(+)-PHNO is a D3 receptor preferring agonist *in vivo*. *Synapse* **60**: 485–495.

Narendran R, Slifstein M, Hwang DR, Hwang Y, Scher E, Reeder S *et al* (2007). Amphetamine-induced dopamine release: duration of action as assessed with the D2/3 receptor agonist radiotracer

(−)-N-[(11)C]propyl-norapomorphine ([^{11}C]NPA) in an anesthetized nonhuman primate. *Synapse* **61**: 106–109.

Okauchi T, Suhara T, Maeda J, Kawabe K, Obayashi S, Suzuki K (2001). Effect of endogenous dopamine on endogenous dopamine on extrastriated [^{11}C]FLB 457 binding measured by PET. *Synapse* **41**: 87–95.

Paspalas CD, Rakic P, Goldman-Rakic PS (2006). Internalization of D2 dopamine receptors is clathrin-dependent and select to dendro-axonic appositions in primate prefrontal cortex. *Eur J Neurosci* **24**: 1395–1403.

Perry SJ, Lefkowitz RJ (2002). Arresting developments in heptahelical receptor signaling and regulation. *Trends Cell Biol* **12**: 130–138.

Rabiner EA, Slifstein M, Nobrega J, Plisson C, Huiban M, Raymond R *et al* (2009). *In vivo* quantification of regional dopamine-D3 receptor binding potential of (+)-PHNO: studies in non-human primates and transgenic mice. *Synapse* **63**: 782–793.

Rees S, Coote J, Stables J, Goodson S, Harris S, Lee MG (1996). Bicistronic vector for the creation of stable mammalian cell lines that predisposes all antibiotic-resistant cells to express recombinant protein. *Biotechniques* **20**: 102–110.

Riccardi P, Li R, Ansari MS, Zald D, Park S, Dawant B *et al* (2006). Amphetamine-induced displacement of [^{18}F] fallypride in striatum and extrastriatal regions in humans. *Neuropsychopharmacology* **31**: 1016–1026.

Searle G, Beaver JD, Comley RA, Bani M, Tziortzi A, Slifstein M *et al*. Imaging dopamine D3 receptors in the human brain with positron emission tomography, [^{11}C]PHNO, and a selective D3 receptor antagonist. *Biol Psychiatry* (in submission).

Slifstein M, Narendran R, Hwang DR, Sudo Y, Talbot PS, Huang Y *et al* (2004). Effect of amphetamine on [^{18}F]fallypride *in vivo* binding to D_2 receptors in striatal and extrastriatal regions of the primate brain: Single bolus and bolus plus constant infusion studies. *Synapse* **54**: 46–63.

Tibbo P, Silverstone PH, McEwan AJ, Scott J, Joshua A, Golberg K (1997). A single photon emission computed tomography scan study of striatal dopamine D2 receptor binding with ^{123}I-epidepride in patients with schizophrenia and controls. *J Psychiatry Neurosci* **22**: 39–45.

Tsao P, Cao T, von Zastrow M (2001). Role of endocytosis in mediating downregulation of G-protein-coupled receptors. *Trends Pharmacol Sci* **22**: 91–96.

van Berckel BN, Kegeles LS, Waterhouse R, Guo N, Hwang DR, Huang Y *et al* (2006). Modulation of amphetamine-induced dopamine release by group II metabotropic glutamate receptor agonist LY354740 in non-human primates studied with positron emission tomography. *Neuropsychopharmacology* **31**: 967–977.

Vickery RG, von Zastrow M (1999). Distinct dynamin-dependent and -independent mechanisms target structurally homologous dopamine receptors to different endocytic membranes. *J Cell Biol* **144**: 31–43.

Volkow ND, Fowler JS, Logan J, Alexoff D, Zhu W, Telang F *et al* (2009). Effects of modafinil on dopamine and dopamine transporters in the male human brain: clinical implications. *JAMA* **301**: 1148–1154.

Volkow ND, Wang GJ, Fowler JS, Logan J, Gatley SJ, Hitzemann R *et al* (1997). Decreased striatal dopaminergic responsiveness in detoxified cocaine-dependent subjects. *Nature* **386**: 830–833.

Wilson AA, McCormick P, Kapur S, Willeit M, Garcia A, Hussey D *et al* (2005). Radiosynthesis and evaluation of [^{11}C]-(+)-4-propyl-3,4,4a,5,6,10b-hexahydro-2H-naphtho[1,2-b][1,4]oxazin-9-ol as a potential radiotracer for *in vivo* imaging of the dopamine D2 high-affinity state with positron emission tomography. *J Med Chem* **48**: 4153–4160.

Supplementary Information accompanies the paper on the Neuropsychopharmacology website (http://www.nature.com/npp)